PHOTOCATALYTIC PROPERTIES OF ZnO/CuO/Ag TERNARY COMPOSITES

Do Duc Tho*, Hoang Xuan Truong, Luong Huu Phuoc
Hanoi University of Science and Technology

ARTICLE INFO

Received: 22/4/2024
Revised: 31/5/2024
Published: 31/5/2024

KEYWORDS

ZnO/CuO/Ag ternary composite
Photocatalytic activity
Congo Red degradation
The intermediary role of Ag
Hydrothermal method

ABSTRACT

In this paper, ZnO/CuO/Ag ternary composites were successfully synthesized by hydrothermal method using $Zn(NO_3)_2.6H_2O$, $Cu(NO_3)_2.3H_2O$ and $AgNO_3$. The composite samples were characterized using X-Ray diffraction (XRD), Scanning Electron Microscopy (SEM) and Raman spectroscopy. Their photocatalytic activities were examined using Congo Red (CR) degradation under Xenon lamp 55 W illumination. The organic dyes degradation was determined by decreasing of characteristic intensity peak in UV-Vis spectrum versus time of their solutions. In comparison with CR, the degradation of other organic dyes such as Methylene Blue (MB), Rhodamine B (RhB) and Crystal Violet (CV) was examined. The result showed that the ZnO/CuO/Ag composite (n_{Cu}^{2+}/n_{Zn}^{2+} = 0.10) exhibited higher photocatalytic activity. The degradation reaches 84.8% when the CR solution with concentration of 10 ppm and 40 mg of this composite was tested. The enhanced photocatalytic activity in mainly attributed to the construction of chemical potential gradients between proper amount of CuO and ZnO adding the intermediary role of Ag.

TÍNH CHẤT QUANG XÚC TÁC CỦA TỔ HỢP BA THÀNH PHẦN ZnO/CuO/Ag

Đỗ Đức Thọ*, Hoàng Xuân Trường, Lương Hữu Phước
Đại học Bách khoa Hà Nội

THÔNG TIN BÀI BÁO

Ngày nhận bài: 22/4/2024
Ngày hoàn thiện: 31/5/2024
Ngày đăng: 31/5/2024

TỪ KHÓA

Tổ hợp ZnO/CuO/Ag
Khả năng quang xúc tác
Phân hủy Congo Red
Vai trò trung gian của Ag
Phương pháp thủy nhiệt

TÓM TẮT

Trong bài báo này, tổ hợp ba thành phần ZnO/CuO/Ag được chế tạo thành công bằng phương pháp thủy nhiệt từ các muối $Zn(NO_3)_2.6H_2O$, $Cu(NO_3)_2.3H_2O$ và $AgNO_3$. Cấu trúc tinh thể, hình thái và tính chất quang của các mẫu vật liệu được xác định qua các phép đo như nhiễu xạ tia X, hiển vi điện tử quét và phổ Raman. Tính chất quang xúc tác của chúng được xác định qua khả năng phân hủy Congo Red (CR) khi được chiếu sáng bởi đèn Xenon có công suất 55 W. Sự phân hủy các chất màu được xác định qua sự giảm cường độ đỉnh đặc trưng trong phổ UV-Vis của các dung dịch chất màu. Để so sánh với CR, các chất màu khác nhau như Methylene Blue (MB), Rhodamine B (RhB) và Crystal Violet (CV) cũng được khảo sát. Kết quả chỉ ra rằng tổ hợp ba thành phần ZnO/CuO/Ag (n_{Cu}^{2+}/n_{Zn}^{2+} = 0,10) thể hiện khả năng quang xúc tác cao nhất. Khả năng phân hủy CR trong dung dịch của mẫu này lên tới 84,8% khi sử dụng 40 mg vật liệu với dung dịch Congo Red 10 ppm. Sự cải thiện khả năng quang xúc tác được cho là do hình thành gradien thế hóa ở tổ hợp với lượng CuO và ZnO thích hợp cộng với vai trò trung gian của Ag.

DOI: https://doi.org/10.34238/tnu-jst.10189

* Corresponding author. *Email: tho.dhbk.teach.2019@gmail.com*

1. Introduction

Zinc oxide (ZnO) has attracted much attention because of its utilities as photocatalyst due to its excellent optical activity, wideband gap of 3.37 eV, large exciton binding energy (60 meV), natural abundance, low cost and environmental friendliness [1] – [3]. However, pure ZnO nanostructures has large band gap energy and high recombination rate of photogenerated electron-hole pairs [4], [5], resulting in exhibiting low application rate for visible light and photocatalytic efficiency, which powerfully affect its practical application. Hence, great efforts were usually used to enhance the photocatalytic activity of ZnO nanostructure, such as decorating, doping, semiconductor compounding, and catalyzer carrier [6], [7].

Among of above mentioned methods, it is very effective for enhancing the photocatalytic activity of ZnO nanostructures to form composite with other semiconductor oxide to improve the sunlight utilization and decrease the recombination of photogenerated electron-hole pairs, resulting in improving the photocatalytic activity of ZnO nanostructures. In great oxide semiconductors, CuO, a p-type semiconductor, could compose ZnO to overcome the limitations due to its narrow band gap energy of 1.20-1.75 eV, good electrical conductivity, non-toxicity, high stability and natural abundance [8]. Different approaches have been selected to prepare ZnO/CuO nanocomposites, such solid-state method [9] thermal oxidation and laser ablation [10] and wet chemical process [11]. Moreover, it has been seen that the noble metal introduction like silver (Ag) on ZnO could widen the absorption spectrum and promote the separation efficiency of electron-hole pairs after excitation [12].

In the article, ZnO/CuO/Ag composites were successfully synthesized by hydrothermal method using $Zn(NO_3)_2.6H_2O$, $Cu(NO_3)_2.3H_2O$ and $AgNO_3$. This method has several advantages such as facile method, low cost, accurate control of stoichiometry, easy realization, fast reaction rate, the quality and purity of the synthesized products, and the obtaining of materials with great variety of crystalline structure [13]. In addition, the hydrothermal method can also be used to receive products in large quantities. Hence, this method was selected to synthesize ZnO/CuO/Ag composites in our group. Their photocatalytic activities were examined using Congo Red (CR) degradation. This article focused on Congo Red dye due to limitation of research reports. The influence of Ag presence on the photocatalytic activity of ZnO/CuO composites was also discussed.

2. Experiment

All the chemicals were of analytical grade without any further purification and processing. To synthesis the ZnO/CuO composites, an amount of $Zn(NO_3)_2.6H_2O$ and a proper amount of $Cu(NO_3)_2.3H_2O$ were respectively dissolved in 100 ml of double-distilled (DI) water under magnetic stirring for 5 min. Next, 0.5 g CTAB (Cetyltrimethylammonium bromid) was added to the mixed solution. When the CTAB was completely dissolved then 2.5 g NaOH was added. After stirring with a magnetic stir for 1 h, the mixed solution was then transferred into a teflon-lined stainless autoclave and heated at 140 ^oC for 3 h. Next, the obtained precipitation was carefully washed and filtered by DI water and absolute ethanol. Lastly, the precipitation was dried at 80 ^oC for 24 h to obtain ZnO/CuO composites.

For synthesis ZnO/CuO/Ag ternary composites, 0.5 g $AgNO_3$ and 0.1 g PVP (Polyvinylpyrrolidone) were dissolved in 30 ml EG (Ethylene Glycol) to form the $AgNO_3$ solution. A proper amount of synthesized above ZnO/CuO was dispersed in 30 ml DI water and magnetically stirred about 30 min. Afterwards, the mix was added the $AgNO_3$ solution under magnetic stirring of 30 min. Next, the mix was transferred into a teflon-lined stainless autoclave and heated at 140 ^oC for 2 h. Finally, the precipitation was selected and dried at 80 ^oC for 24 h. The prepared ZnO/CuO/Ag composite samples are presented in Table 1.

Table 1. *The prepared ZnO/CuO/Ag composites*

Sample	Concentration ratio (n_{Cu}^{2+}/n_{Zn}^{2+})	$AgNO_3$ (g)
M5	1%	0.5
M7	3%	0.5
M10	5%	0.5
M15	7%	0.5

The morphology of the samples was determined by scanning electron microscopy (SEM, Tabletop Microscope TM4000 Plus, Hitachi). Their structures were examined by a powder X-ray diffractometer (XRD) with CuKα radiation (X'pert Pro, PANalytical). The Raman spectra of the samples were recorded with a Raman microscope (Renishaw Invia Raman Microscope). Their UV-Vis spectra were recorded by a UV-Vis spectrometer (Jasco V-750). All measurements were performed at room temperature.

The highest degradation efficiency was calculated as in following equation (1):

$$H = \frac{C_0 - C_t}{C_0} \times 100\% = \frac{I_0 - I_t}{I_0} \times 100\% \quad (1)$$

Where C_0, C_t are the initial concentration and concentration after photodegradation, respectively. I_0 and I_t are the initial absorption intensity and the absorption intensity after photodegradation of dye solution and H is the degradation efficiency of dye.

3. Results and discussion

SEM image of the M10 sample was depicted in Figure 1. We can observe different particles mixed with rods. The formed rods with average length of several μm and diameter of about μm mixed with average diameter of hundreds nm particles. In addition, we can observe some picture places brighter than others. These places can be contributed to presences of Ag particles.

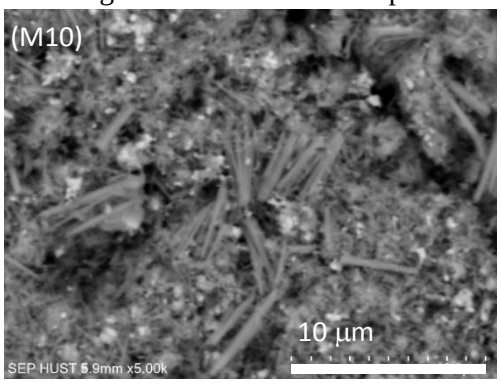

Figure 1. *SEM images of the samples*

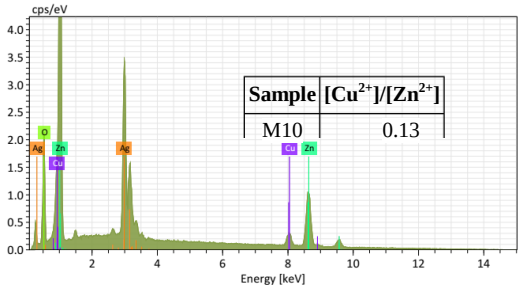

Figure 2. *EDX spectrum of the samples*

EDX spectrum of this sample (Figure 2) depicts that all elements Zn, Cu, O and Ag were presented. Moreover, the composition obtained from the EDX spectrum, which is depicted in the inset, is roughly consistent with the desired weight ratio CuO and ZnO.

Figure 3 depicts the XRD pattern of the samples. The results depict that all intensive diffraction peaks in the patterns are indexed to hexagonal structure of ZnO with lattice constant of $a = b = 0.3249$ nm and $c = 0.5206$ nm (JCPDS 36-1451). The diffraction peak at 38.1^o can be indexed to the monoclinic of CuO (JCPDS 45-0937). Other peaks can be indexed to face-centered cubic Ag (JCPDS 04-0783).

The Raman spectrum of the M10 sample (Figure 4) shows the peaks at 430 and 582 cm^{-1} for hexagonal wurtzite structure of ZnO. The peak at 582 cm^{-1}, situated between A_1 (LO) and E_1 (LO) optical phonon mode, assigned to the oxygen imperfection. The peak at 382 cm^{-1} is assigned to A_1 transverse mode and existed from the anisotropic nature in the force constant. The

peak at 348 cm^{-1} for monoclinic CuO. Among these, the peak at 348 cm^{-1} was assigned to A_g mode and the remaining were to B_g mode. The peak 515 cm^{-1}, possibly related to an overlap of 2(LA) and $2B_1^{low}$ overtones [14] – [20].

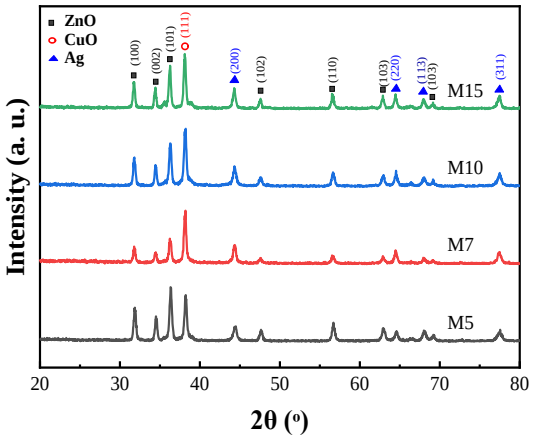

Figure 3. *XRD patterns of the samples*

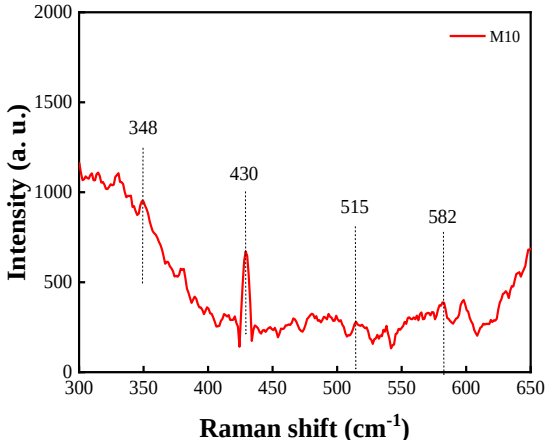

Figure 4. *Raman spectra of the M10 sample*

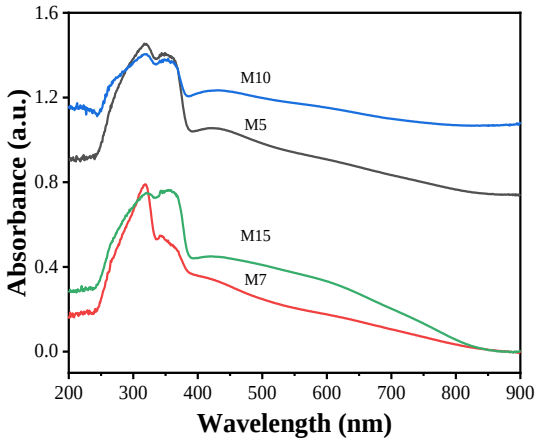

Figure 5. *Absorption spectra of the samples*

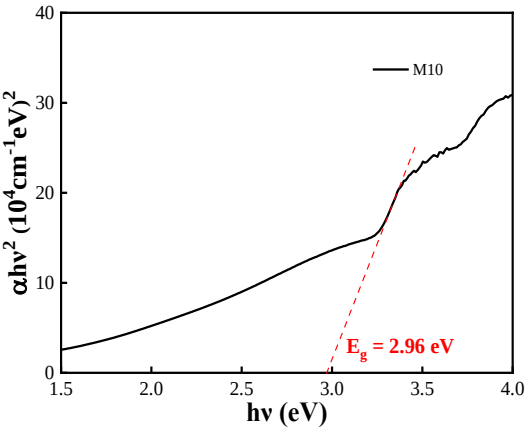

Figure 6. *Method of band gap energy E_g determination from the Tauc plot. The linear part of the plot is extrapolated to the x-axis*

Figure 5 depicts UV-Vis absorption spectra of the composite samples. We can observe that the edge absorption is nearly 400 nm, which is in accordance with the values in the literature. The reported values for the absorption edge of ZnO are in the range of 380-400 nm [21], [22]. The absorption of the samples decreased lightly with increasing light wavelength. However, it can be seen that the M10 sample depicts the best absorption in the visible light region. Hence, its light conversion increases, resulting in growth of photocatalytic activity.

The optical band gap of the M10 sample, which was determined by modified Kubelka – Munk function, is depicted in Figure 6. The mathematical relation between the photon energy $h\nu$ and α for allowed transition is following:

$$[\alpha h\nu]^{1/\gamma} = A(h\nu - E_g) \quad (2)$$

Where α is the energy-dependent absorption coefficient, h is the Planck constant, ν is the photon's frequency, E_g is the optical band gap energy, A is a constant, γ factor depends on the nature of the electron transition and is equal to 1/2 or 2 for the direct and indirect transition band

gaps, respectively. In this report, the γ factor was taken value 1/2 resulting the optical band gap of the M10 sample is 2.96 eV.

The photocatalytic performance of the samples with the weight of 30 mg under Xenon lamp illumination was evaluated using CR solution with a concentration of 10 ppm as the organic pollutant was depicted in Figure 7. After 150 min, the M10 sample depicts the highest degradation efficiency (76.8 %) (Table 2). Hence, the M10 sample was chosen to other experiments.

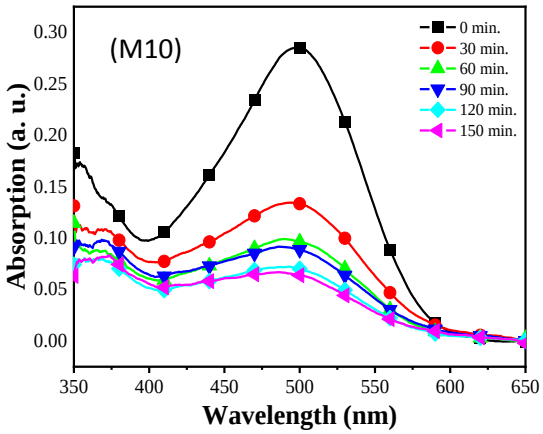

Figure 7. *The CR degradation of the samples*

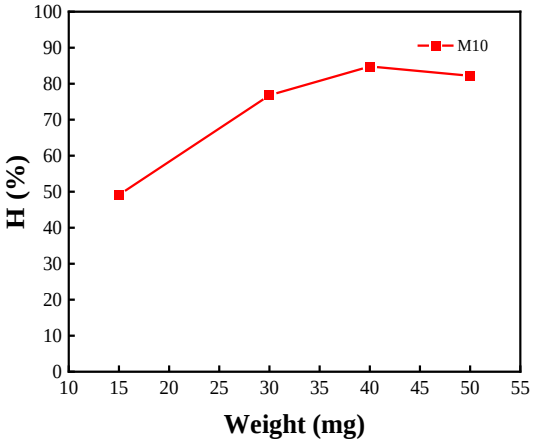

Figure 8. *The influence of weight on the M10 sample degradation efficiency*

Table 2. *Degradation efficiency of the samples with weight of 30 mg and the CR solution of 10 ppm*

Sample	H (%)
M5	56.8
M7	32.4
M10	76.8
M15	54.2

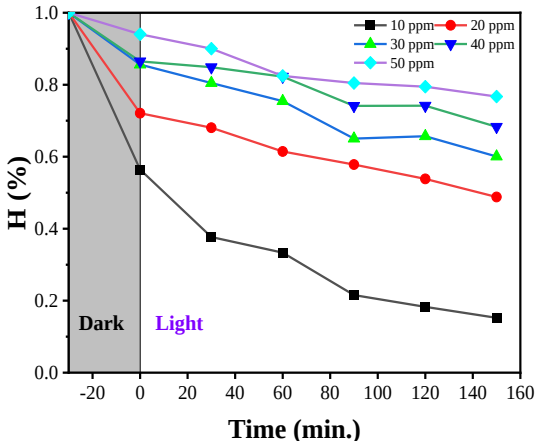

Figure 9. *The M10 sample degradation efficiency on concentration*

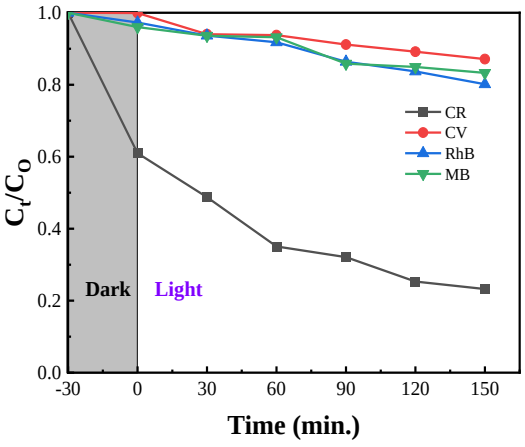

Figure 10. *The degradation of M10 sample versus differential dyes*

Figure 8 depicts the M10 sample degradation efficiency of its weight. The degradation of the M10 sample reaches the largest value when it weight is 40 mg. It was unchanged with increase of weight of the M10 sample. Therefore, the weight of 40 mg was used for the next experiments. In sequence, the M10 sample degradation dependency of concentration was examined. The CR

solution concentrations of 10, 20, 30 and 50 ppm were selected. The result of this experiment is depicted in Figure 9. It can be seen that the optimum concentration is 10 ppm.

In comparison, the CR, CV, RhB, MB solutions of 10 ppm of concentration were taken for examination. The M10 sample with 40 mg of weight was used for each solution. Figure 10 depicts that the degradation rate of M10 sample is the highest for CR. The value is 84.8%.

A charge transfer mechanism during photocatalytic reactions could be proposed according to the radical scavenging results. The reported values of the conduction band for CuO and ZnO are approximately -0.92 and -0.27 eV, respectively [23]. Hence, the ZnO and CuO valence bands could estimate to be 3.10 and 0.28 eV, respectively. Figure 11 depicts the schematic of the charge transfer process during photocatalytic reactions over the samples under Xenon light radiation. After photoexcitation (Eq. (3)), the electrons in the ZnO conduction band recombine with the holes in the CuO conduction band through the Z-scheme mechanism due to the interfacial electric field (Eq. (4)) [24]. At the same time, as shown in Eq. (5), the electrons in the CuO conduction band have enough potential (more negative than - 0.33 eV) to create superoxide radicals. Holes in the valence band of ZnO could oxidize water to produce hydroxyl radicals due to the more positive valence band than 2.38 eV (Eq. (6)) [25]. Hence, in accordance with the radical scavenging results, the superoxide and hydroxyl radicals are the main active species in the photocatalytic reactions over the samples (Eqs. (11) and (12). Hence, Ag loading could facilitate the recombination process Eqs. (7)-(9) due to the Schottky barrier formation at the metal-semiconductor interface. Band bending in the ZnO-Ag interface leads to the electron migration from the ZnO conduction band to Ag. The main reason for this phenomenon is a more positive Fermi level of the Ag compared to the ZnO conduction band [26]. Simultaneously, the created holes migrate from the CuO valence band to Ag. Hence, Ag can act as an electron mediator for the recombination of the electron-hole pairs with low reduction-oxidation potential. Additionally, the photoexcited electrons could migrate from the CuO conduction band to Ag due to the work function difference between CuO and Ag (Eq. (10)) [27]. It has been reported that oxygen could be chemisorbed on Ag. So, the trapped photoexcited electrons by Ag react readily with oxygen due to the low activation energy [24]. Hence, the role of the Ag during photocatalytic reactions over the samples might be as follows: i) recombination center for annihilating electrons in the ZnO conduction band and holes in the CuO valence band; ii) electron capturing from the conduction band of the CuO for producing superoxide radicals. The proposed pathway for the samples could be as follows [28]:

$$\mathrm{ZnO/CuO} + h\nu = \mathrm{ZnO}(h_{\mathrm{VB}}, e_{\mathrm{CB}}) + \mathrm{CuO}(h_{\mathrm{VB}}, e_{\mathrm{CB}}) \quad (3)$$

$$\mathrm{ZnO}(e_{\mathrm{CB}}) + \mathrm{CuO}(h_{\mathrm{VB}}) \rightarrow \text{recombination} \quad (4)$$

$$\mathrm{CuO}(e_{\mathrm{CB}}) + \mathrm{O_2} \rightarrow \bullet\mathrm{O_2^-} \quad (5)$$

$$\mathrm{ZnO}(h_{\mathrm{VB}}) + \mathrm{H_2O} \rightarrow \bullet\mathrm{OH} \quad (6)$$

$$\mathrm{ZnO}(e_{\mathrm{CB}}) + \mathrm{Ag} \rightarrow \mathrm{ZnO{+}Ag}(e_{\mathrm{ZnO}}) \quad (7)$$

$$\mathrm{CuO}(h_{\mathrm{VB}}) + \mathrm{Ag} \rightarrow \mathrm{CuO{+}Ag}(h_{\mathrm{CuO}}) \quad (8)$$

$$\mathrm{Ag}(e_{\mathrm{ZnO}}) + \mathrm{Ag}(h_{\mathrm{CuO}}) \rightarrow \text{recombination} \quad (9)$$

$$\mathrm{Ag}(e_{\mathrm{CuO}}) + \mathrm{O_2} \rightarrow \bullet\mathrm{O_2^-} \quad (10)$$

$$\bullet\mathrm{O_2^-} + \mathrm{CR} + \text{intermediates} \rightarrow \text{degraded products} \quad (11)$$

$$\bullet\mathrm{OH} + \mathrm{CR} + \text{intermediates} \rightarrow \text{degraded products} \quad (12)$$

These results suggest that Ag compositing in the ZnO-CuO composite improved the charge transfer more effectively through a low resistance mediator, which agrees with the obtained photodegradation efficiency and radical scavenging experiment of the samples.

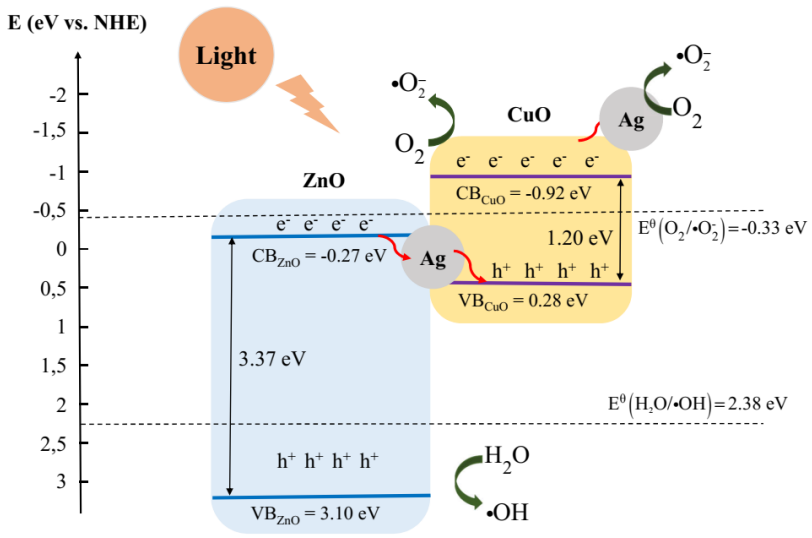

Figure 11. *Mechanism of CR molecule degradation*

4. Conclusion

In summary, we have presented a hydrothermal method for the synthesis of ZnO/CuO/Ag ternary composites. The sample M10 (n_{Cu}^{2+}/n_{Zn}^{2+} = 0.10) exhibited the highest photocatalytic activity. These results also show that the M10 sample may be a promising material to photocatalytic processes.

Acknowledgements

This research is funded by Hanoi University of Science and Technology (HUST) under project number T2022-PC-058.

REFERENCES

[1] K. K. Supin, P. N. P. Namboothiri, and M. Vasundhara, "Enhanced photocatalytic activity in ZnO nanoparticles developed using novel Lepidagathis ananthapuramensis leaf extract," *RSC Adv.*, vol. 13, no. 3, pp. 1497–1515, 2023.

[2] K. R. Ahammed, M. Ashaduzzaman, S. C. Paul, M. R. Nath, S. Bhowmik, O. Saha, M. M. Rahaman, S. Bhowmik, and T. D. Aka, "Microwave assisted synthesis of zinc oxide (ZnO) nanoparticles in a noble approach: utilization for antibacterial and photocatalytic activity," *SN Appl. Sci.*, vol. 2, no. 5, pp. 1–14, 2020.

[3] P. Singh, R. Kumar, and R.K. Singh, "Progress on Transition Metal-Doped ZnO Nanoparticles and Its Application," *Ind. Eng. Chem. Res.*, vol. 58, no. 37, pp. 17130–17163, 2019.

[4] E. Cerrato, N. Paulo, F. Gonçalves, P. Calza, and M. C. Paganini, "Comparison of the Photocatalytic Activity of A Mechanicistic Approach," *Catalysts*. vol. 10, no. 1222, pp. 1–15, 2020.

[5] H. Huan, H. Jile, Y. Tang, X. Li, Z. Yi, X. Gao, X. Chen, J. Chen, and P. Wu, "Fabrication of ZnO@Ag@Ag_3PO_4 ternary heterojunction: Superhydrophilic properties, antireflection and photocatalytic properties," *Micromachines*. vol. 11, no. 3, p. 309, 2020.

[6] T. Chankhanittha, N. Komchoo, T. Senasu, J. Piriyanon, S. Youngme, K. Hemavibool, and S. Nanan, "Silver decorated ZnO photocatalyst for effective removal of reactive red azo dye and ofloxacin antibiotic under solar light irradiation," *Colloids Surfaces A Physicochem. Eng. Asp.*, vol. 626, p. 127034, May 2021.

[7] Z. Mirzaeifard, Z. Shariatinia, M. Jourshabani, and S.M. R. Darvishi, "ZnO Photocatalyst Revisited: Effective Photocatalytic Degradation of Emerging Contaminants Using S-Doped ZnO Nanoparticles under Visible Light Radiation," *Ind. Eng. Chem. Res.*, vol. 59, no. 36, pp. 15894–15911, 2020.

[8] A. Lavín, R. Sivasamy, E. Mosquera, and M.J. Morel, "High proportion ZnO/CuO nanocomposites: Synthesis, structural and optical properties, and their photocatalytic behavior," *Surfaces and Interfaces*,

vol. 17, p. 100367, 2019.
[9] N. Kumaresan, M. M. A. Sinthiya, K. Ramamurthi, R. R. Babu, and K. Sethuraman, "Visible light driven photocatalytic activity of ZnO/CuO nanocomposites coupled with rGO heterostructures synthesized by solid-state method for RhB dye degradation," *Arab. J. Chem.*, vol. 13, no. 2, pp. 3910–3928, 2020.
[10] A. A. Baroot, M. Alheshibri, Q. A. Drmosh, S. Akhtar, E. Kotb, and K. A. Elsayed, "A novel approach for fabrication ZnO/CuO nanocomposite via laser ablation in liquid and its antibacterial activity: A novel approach for fabrication ZnO/CuO nanocomposite," *Arab. J. Chem.*, vol. 15, no. 2, p. 103606, 2022.
[11] R. M. Mohamed and A.A. Ismail, "Photocatalytic reduction and removal of mercury ions over mesoporous CuO/ZnO S-scheme heterojunction photocatalyst," *Ceram. Int.*, vol. 47, no. 7, pp. 9659–9667, 2021.
[12] M. Ahmad, W. Rehman, M. M. Khan, M. T. Qureshi, A. Gul, S. Haq, R. Ullah, A. Rab, and F. Menaa, "Phytogenic fabrication of ZnO and gold decorated ZnO nanoparticles for photocatalytic degradation of Rhodamine B," *J. Environ. Chem. Eng.*, vol. 9, no. 1, p. 104725, 2021.
[13] E. Suvaci and E. Özel, "Hydrothermal Synthesis," *Encycl. Mater. Tech. Ceram. Glas.*, vol. 1-3, pp. 59-68, 2021.
[14] S. S. A. K. Bhunia, P. K. Jha, and D. Rout, "Morphological Properties and Raman Spectroscopy of ZnO Nanorods," *J. Phys. Sci.*, vol. 21, pp. 111–118, December 2016.
[15] A. Sharma, B. P. Singh, S. Dhar, A. Gondorf, and M. Spasova, "Effect of surface groups on the luminescence property of ZnO nanoparticles synthesized by sol-gel route," *Surf. Sci.*, vol. 606, no. 3–4, pp. L13–L17, 2012.
[16] A.S. Nazir, Z. Imran, A. Malik, M. Nazir, M.W. Ashraf, and S. Tayyaba, "Microwave assisted pH controlled ZnO morphology," *Dig. J. Nanomater. Biostructures*, vol. 13, no. 1, pp. 307–313, 2018.
[17] J. Fang and Y. Xuan, "Investigation of optical absorption and photothermal conversion characteristics of binary CuO/ZnO nanofluids," *RSC Adv.*, vol. 7, no. 88, pp. 56023–56033, 2017.
[18] P. Sriyutha Murthy, V. P. Venugopalan, D. D. Arunya, S. Dhara, R. Pandiyan, and A. K. Tyagi, "Antibiofilm activity of nano sized CuO," *Proc. Int. Conf. Nanosci. Eng. Technol. ICONSET 2011*, 2011, pp. 580–583.
[19] A. B. Bodade, M.A. Taiwade, and G. N. Chaudhari, "Bioelectrode based chitosan-nano copper oxide for application to lipase biosensor," *J. Appl. Pharm. Res.*, vol. 5, no. 1, pp. 30–39, 2017.
[20] N. F. Santos, J. Rodrigues, S. O. Pereira, A. J. S. Fernandes, T. Monteiro, and F. M. Costa, "Electrochemical and photoluminescence response of laser-induced graphene/electrodeposited ZnO composites," *Sci. Rep.*, vol. 11, no. 1, p. 17154, 2021.
[21] C. Zhang, W. Fei, H. Wang, N. Li, D. Chen, Q. Xu, H. Li, J. He, and J. Lu, "p-n Heterojunction of BiOI/ZnO nanorod arrays for piezo-photocatalytic degradation of bisphenol A in water," *J. Hazard. Mater.*, vol. 399, p. 123109, May 2020.
[22] X. Ding, K. Lin, Y. Li, M. Dang, and L. Jiang, "Synthesis of Biocompatible Zinc Oxide (ZnO) Nanoparticles and Their Neuroprotective Effect of 6-OHDA Induced Neural Damage in SH-SY 5Y Cells," *J. Clust. Sci.*, vol. 31, no. 6, pp. 1315–1328, 2020.
[23] S. Ruan, W. Huang, M. Zhao, H. Song, and Z. Gao, "A Z-scheme mechanism of the novel ZnO/CuO n-n heterojunction for photocatalytic degradation of Acid Orange 7," *Mater. Sci. Semicond. Process.*, vol. 107, p. 104835, 2020.
[24] H. Yu, J. Huang, L. Jiang, L. Leng, K. Yi, W. Zhang, C. Zhang, and X. Yuan, "In situ construction of Sn-doped structurally compatible heterojunction with enhanced interfacial electric field for photocatalytic pollutants removal and CO_2 reduction," *Appl. Catal. B Environ.*, vol. 298, p. 120618, 2021.
[25] D. Huang, S. Chen, G. Zeng, X. Gong, C. Zhou, M. Cheng, W. Xue, X. Yan, and J. Li, "Artificial Z-scheme photocatalytic system: What have been done and where to go?" *Coord. Chem. Rev.*, vol. 385, pp. 44–80, 2019.
[26] N. Güy and M. Özacar, "The influence of noble metals on photocatalytic activity of ZnO for Congo red degradation," *Int. J. Hydrogen Energy*, vol. 41, no. 44, pp. 20100–20112, 2016.
[27] K. Xu, J. Wu, C.F. Tan, G.W. Ho, A. Wei, and M. Hong, "Ag-CuO-ZnO metal-semiconductor multiconcentric nanotubes for achieving superior and perdurable photodegradation," *Nanoscale*, vol. 9, no. 32, pp. 11574–11583, 2017.
[28] S. Wang, B. Zhu, M. Liu, L. Zhang, J. Yu, and M. Zhou, "Direct Z-scheme ZnO/CdS hierarchical photocatalyst for enhanced photocatalytic H2-production activity," *Appl. Catal. B Environ.*, vol. 243, pp. 19–26, 2019.